

*Electronic Supplementary Information (ESI) for*

# **Chiral Mesostructured Hydroxide Zinc Carbonate for Enantioseparation in High Performance Liquid Chromatography**

Lin Li,<sup>[a]</sup> Zexi Liu,<sup>[a]</sup> Lu Han,<sup>[a]</sup> Shunai Che,<sup>\*,[a,b]</sup> Yingying Duan<sup>\*,[a]</sup>

<sup>[a]</sup> School of Chemical Science and Engineering, Tongji University, 1239 Siping Road, Shanghai, P. R. China. E-mail: yyduan@tongji.edu.cn.

<sup>[b]</sup> School of Chemistry and Chemical Engineering, State Key Laboratory of Composite Materials, Shanghai Key Laboratory for Molecular Engineering of Chiral Drugs, Shanghai Jiao Tong University, 800 Dongchuan Road, Shanghai, P. R. China. E-mail: chesa@sjtu.edu.cn.

## **Table of Contents**

### **Experimental Section**

**Figure S1. SEM images of L-CMHZC@S synthesized with different hydrothermal time of 0.5 h (a), 1.0 h (b), 1.5 h (c), 2.0 h (d), 2.5 h (e) and 3.0 h (f).**

**Figure S2. The EDAX analysis for the original silica gel (a), manganese-activated silica gel (b), and L-CMHZC@S with varying magnification (c<sub>1-2</sub>).**

**Figure S3. Raman spectra of L-Met and L-CMHZC@S.**

**Figure S4. TGA (a) and MS (b) of L-CMHZC@S.**

**Figure S5. The DLS analysis of silica gel and L-CMHZC@S.**

**Figure S6. Side view of L-CMHZC@S in Fig. 1c.**

**Figure S7. XRD patterns of silica gel and D-CMHZC@S.**

**Figure S8. SEM images of D-CMHZC@S with varying magnifications.**

**Figure S9. DRUV-Vis and DRCD spectra of L- and D-CMHZC@S and raw silica gel (a) and methionine (b).**

**Figure S10. Illustration of driving force for assembling hierarchically chiral structures of L-CMHZC@S.**

**Figure S11. Chromatograms of  $\alpha$ -Phenylethylamine (PA), 2-Chloropropionic acid (CA), 1-Phenyl-1,2-ethanediol (PE) with S-enantiomer and R-enantiomer.**

**Figure S12. Chromatograms of  $\alpha$ -Phenylethylamine (PA) with different injection volume and five repeated injections.**

**Table S1. Comparison of the separation factors among previous published hybrid materials and L-CMHZC@S.**

## Experimental Section

### Materials

Silica gel were purchased from SuZhou NanoMicro Technology Co., Ltd.  $\text{KMnO}_4$  and  $(\text{NH}_4)_2\text{CO}_3$  were purchased from the Sinopharm Chemical Reagent Co., Ltd,  $\text{Zn}(\text{CH}_3\text{OO})_2 \cdot 2\text{H}_2\text{O}$  and L/D-Methionine were purchased from the Macklin Biochemical Co., Ltd. HPLC grade n-hexane and isopropanol were purchased from Adamas Co., Ltd. All chemicals were used as received without further purification.

### Silica gel Activation

Before the hydrothermal process, the silica gel was pretreated as following: silica gel was firstly dissolved in 20 mL (0.04-20 mM) of fresh  $\text{KMnO}_4$  solution, after which 50  $\mu\text{L}$  of *n*-butanol was added as a reducing agent for the  $\text{KMnO}_4$  for 20 to 25 minutes at 80 °C. The permanganate-treated silica gel was washed and treated with deionised water and finally dried at 80 °C.

### Synthesis of CMHZC@Silica gel

The synthesis molar composition was 1.0 L - methionine : 1.5  $\text{Zn}(\text{CH}_3\text{OO})_2$  : 0.5  $(\text{NH}_3)_2\text{CO}_3$  : 1389  $\text{H}_2\text{O}$  : 0.85 silica gel. In a typical synthesis, 1.5 mmol methionine was dissolved in 25 mL of ultrapure water with stirring, and then, 3.0 mmol  $\text{Zn}(\text{CH}_3\text{OO})_2 \cdot 2\text{H}_2\text{O}$  was added to obtain a homogeneous solution, which was allowed to react at 0 °C before adding activated silica gel. After the addition of 1 mmol ammonium carbonate and stirring for 60 min, the mixture of solution and activated silica gel were transferred into 50 mL Teflon-lined autoclaves to react under static conditions at 120 °C for 2 h. The white powder was collected by centrifugation, washed with ultrapure water and freeze dry overnight.

### Characterizations

The morphology of samples were observed with scanning electron microscope (SEM, JEOL JSM-7900) fitted with EDAX apparatus with an accelerating voltage of 5.0 kV and JSM-7100F with an accelerating voltage of 1.0 kV. X-ray powder diffraction (XRD) patterns were recorded on a MiniFlex 600 powder diffractometer equipped with  $\text{Cu K}\alpha$  radiation ( $\lambda = 0.154178$  nm, 40 kV, 15mA). The sample for TEM observations was prepared by peening and sonicating in ethanol. The sectional sample was prepared by slicing of the CMHZC@S sample embedded in epoxy resin. TEM observations were performed using a JEOL JSM-F200 microscope. The DRCD measurements were

obtained using JASCO J-1500 spectropolarimeter fitted with a DRCD apparatus. Raman spectra were measured on a Renishaw Raman spectrometer using 514 nm laser with power of 20 mW. Parameters: 100-4000  $\text{cm}^{-1}$ , step 0.2  $\text{cm}^{-1}$ , integration time 10 s. The thermogravimetric analysis (TGA) and mass spectrum (MS) were measured on the TGA8000-Frontier-Clarus 680-Clarus SQ 8T with a heating rate of 50  $^{\circ}\text{C}\cdot\text{min}^{-1}$ . Dynamic light scattering (DLS) were measured on the Litesizer 500. Chromatographic analysis were conducted on a Dionex Ultimate TM 3000 HPLC equipped with an LGP-3400SD quaternary pump, a WPS-3000 auto-sampler and a VWD-3x00(RS) detector. Chromeleon 7 Chromatography Data System Software (TermoFisher Scientific) was used for the acquisition, monitoring and treatment of data. The wavelength was set at 220 nm and 254 nm. The injection volume of the samples was kept at 10.0  $\mu\text{L}$ .

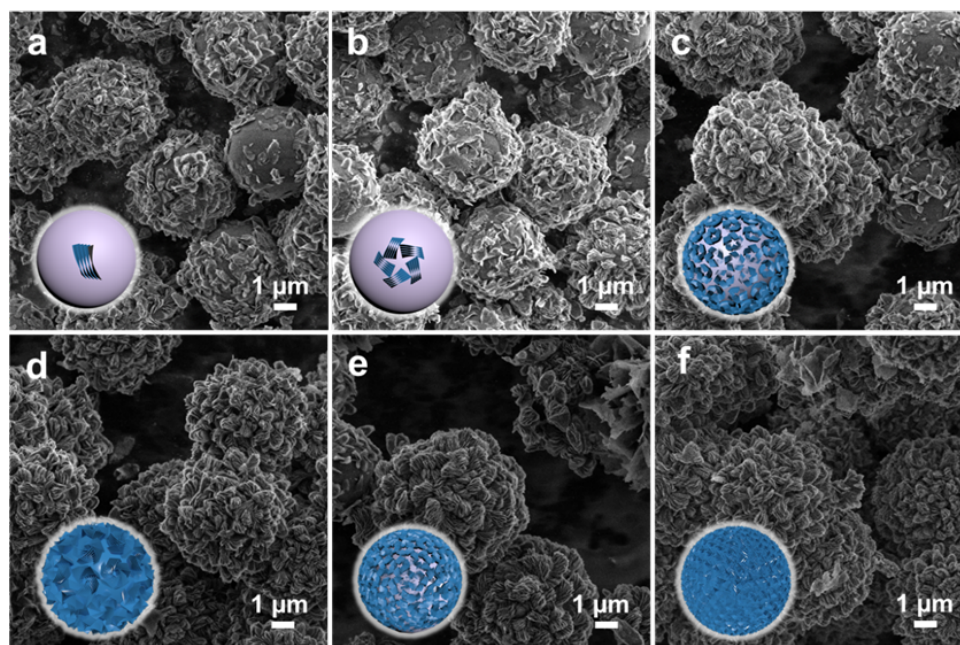


**Figure S1. SEM images of L-CMHZC@S synthesized with different hydrothermal time of 0.5 h (a), 1.0 h (b), 1.5 h (c), 2.0 h (d), 2.5 h (e) and 3.0 h (f).**

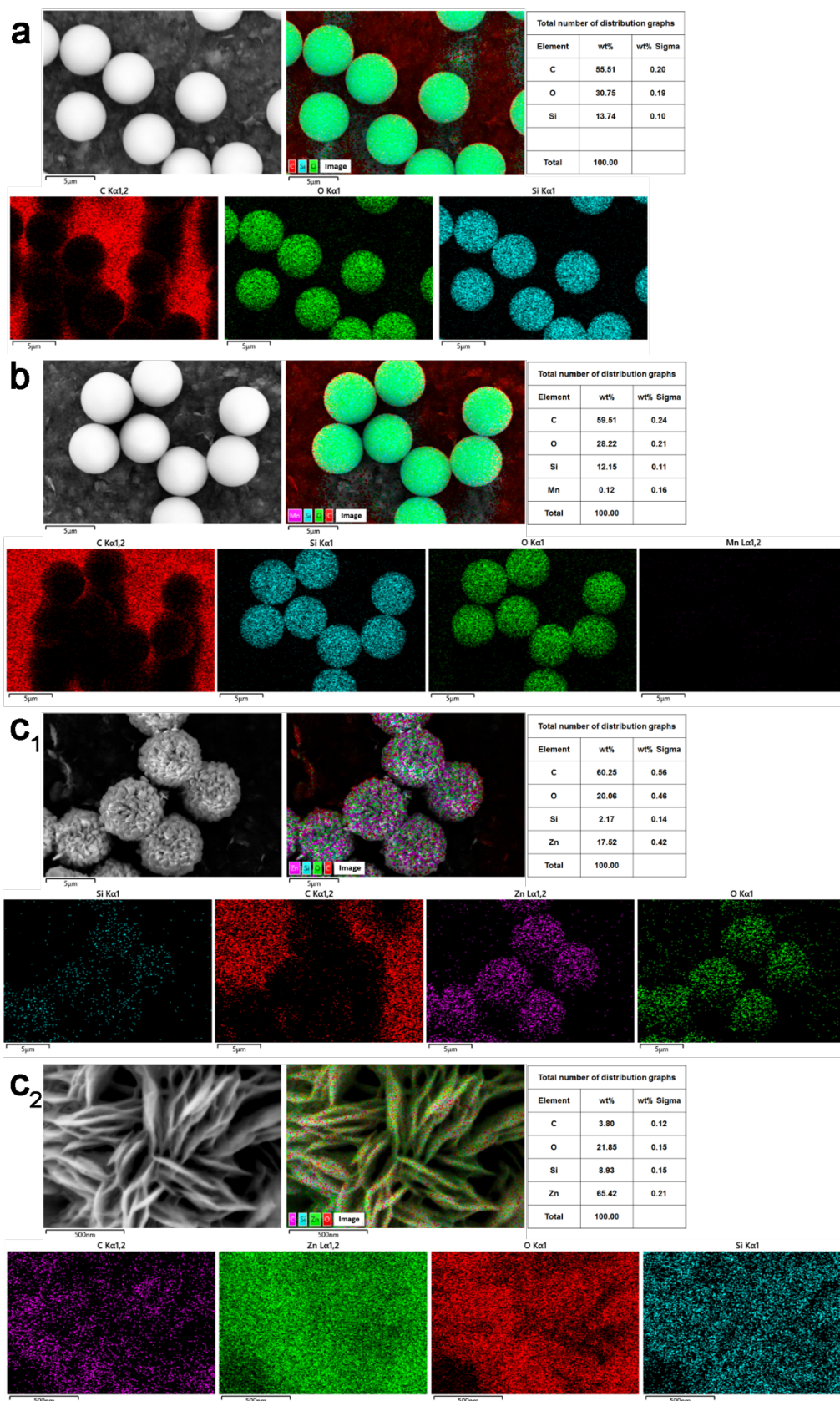


**Figure S2. The EDAX analysis for the original silica gel (a), manganese-activated silica gel (b), and L-CMHZC@S with varying magnification (c<sub>1-2</sub>).**

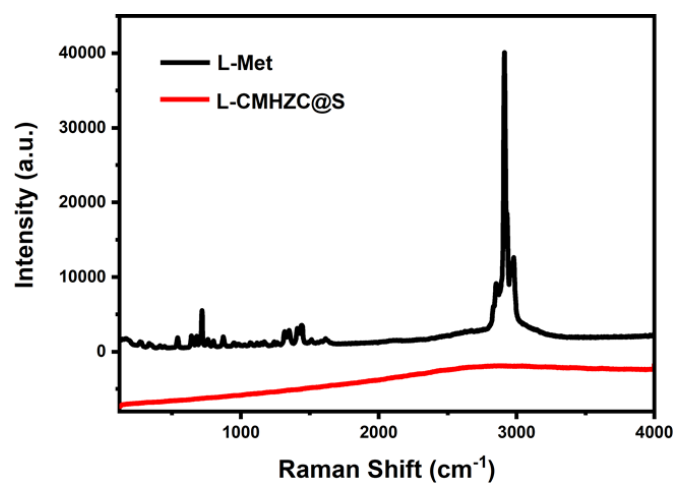


**Figure S3. Raman spectra of L-Met and L-CMHZC@S.**

Raman shifts at 688, 803, 1576, 2541, 2889, 2956, 3012  $\text{cm}^{-1}$  are corresponding to N-H bending in Met. These signals cannot be observed in the L-CMHZC@S sample, indicating the very low organic molecules content in the L-CMHZC@S.

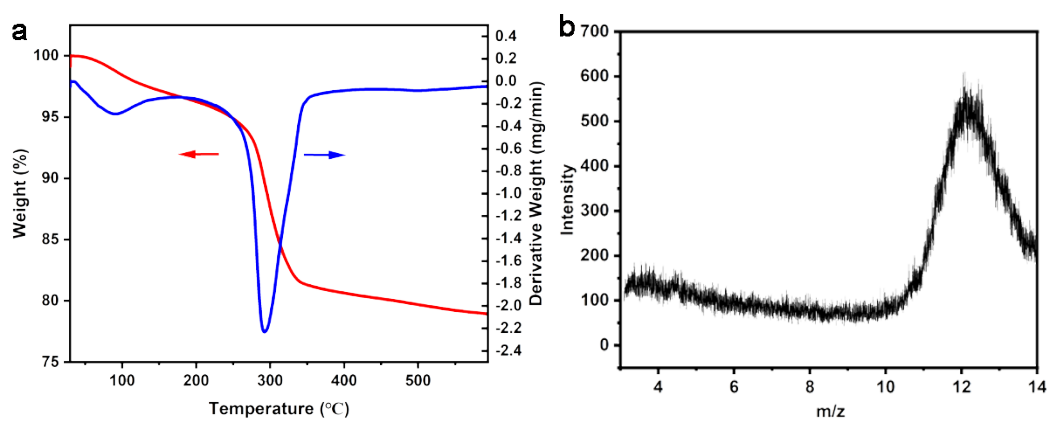


**Figure S4. TGA (a) and MS (b) of L-CMHZC@S.**

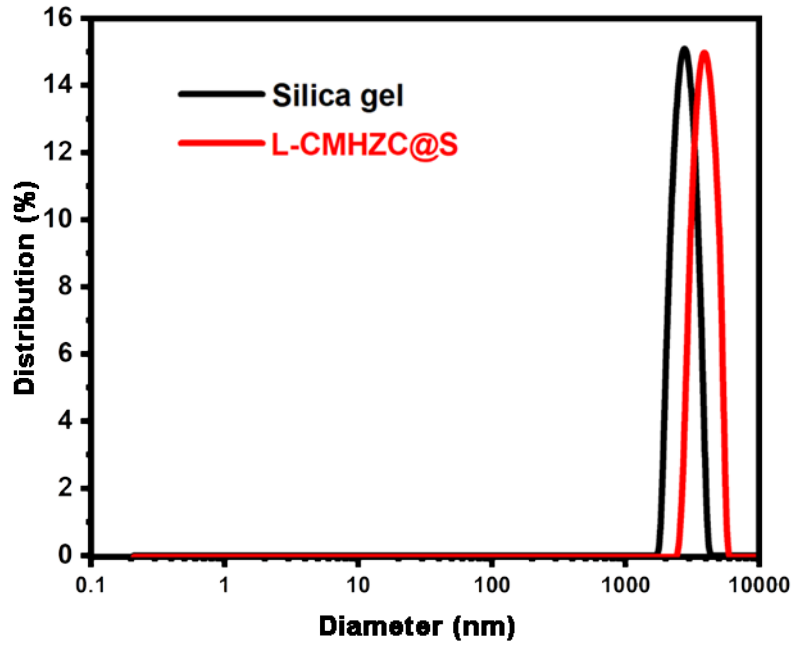


Figure S5. The DLS analysis of silica gel and L-CMHZC@S.

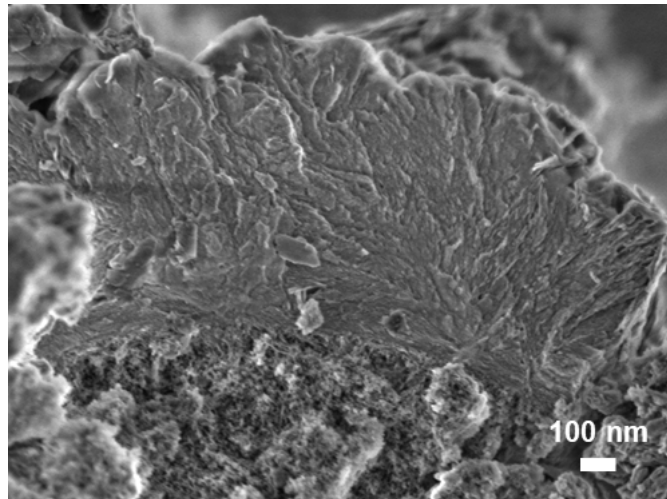


Figure S6. Side view of L-CMHZC@S in Fig. 1c.

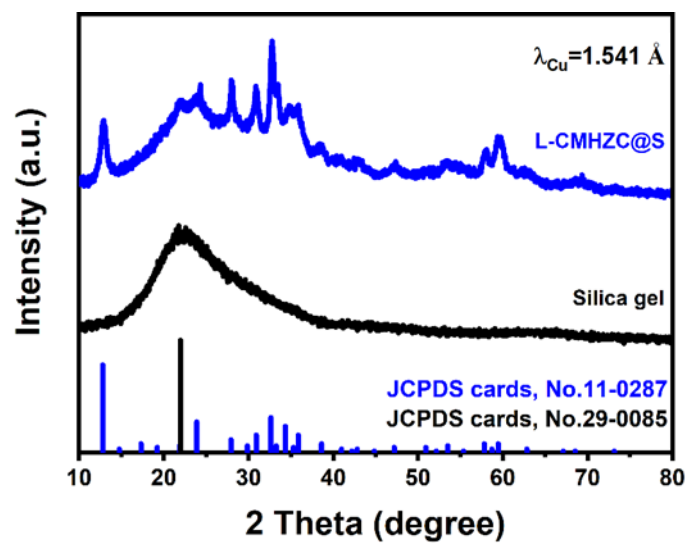


Figure S7. XRD patterns of silica gel and D-CMHZC@S.

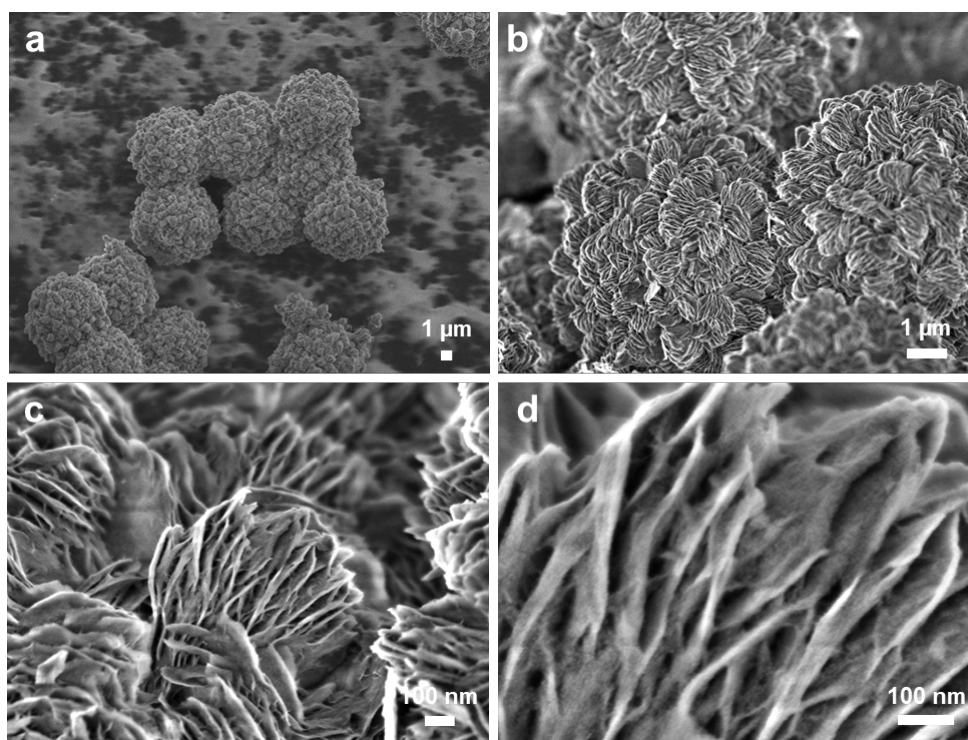


Figure S8. SEM images of D-CMHZC@S with varying magnifications.



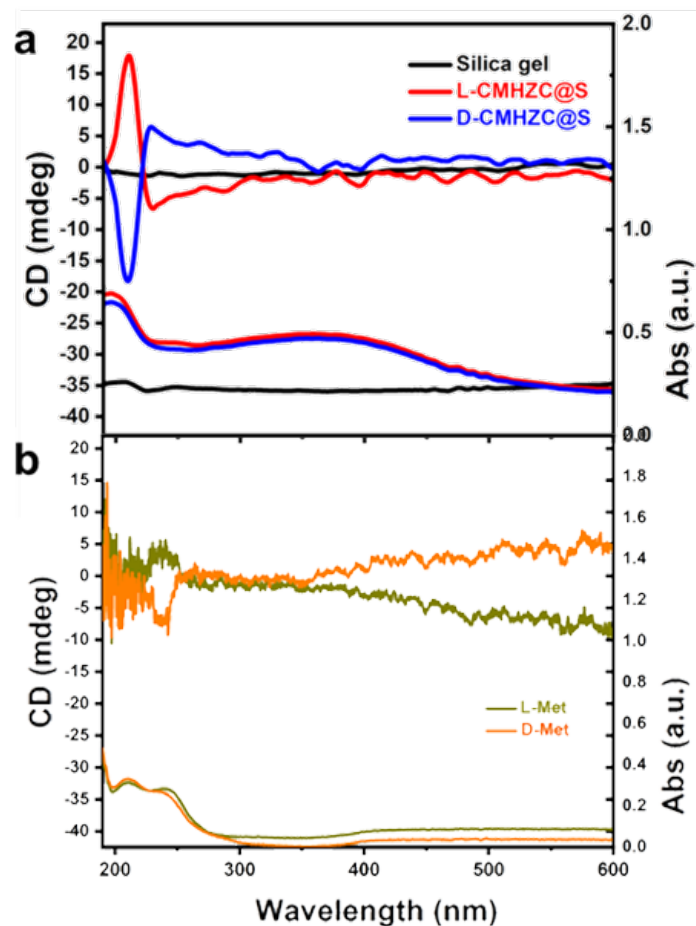


Figure S9. DRUV-Vis and DRCD spectra of L- and D-CMHZC@S and raw silica gel (a) and methionine (b).

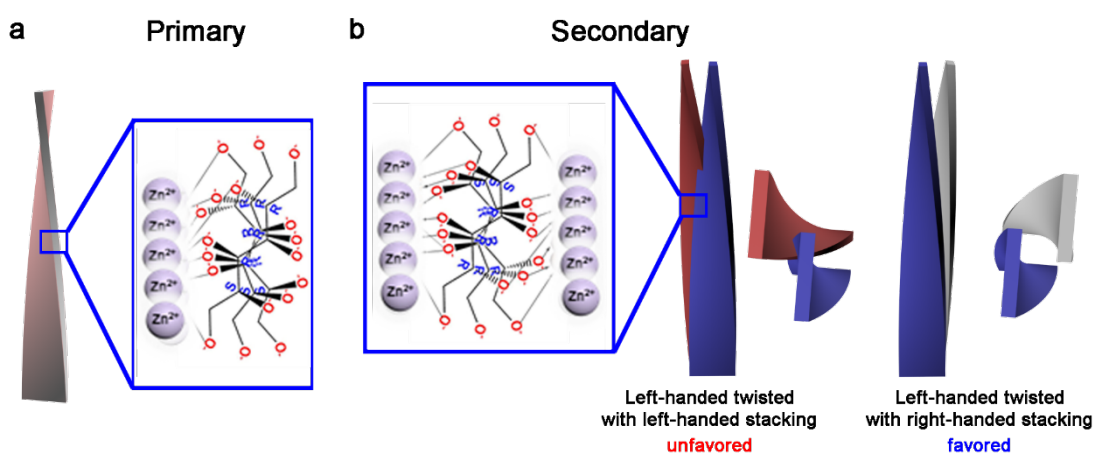


Figure S10. Illustration of driving force for assembling hierarchically chiral structures of L-CMHZC@S.

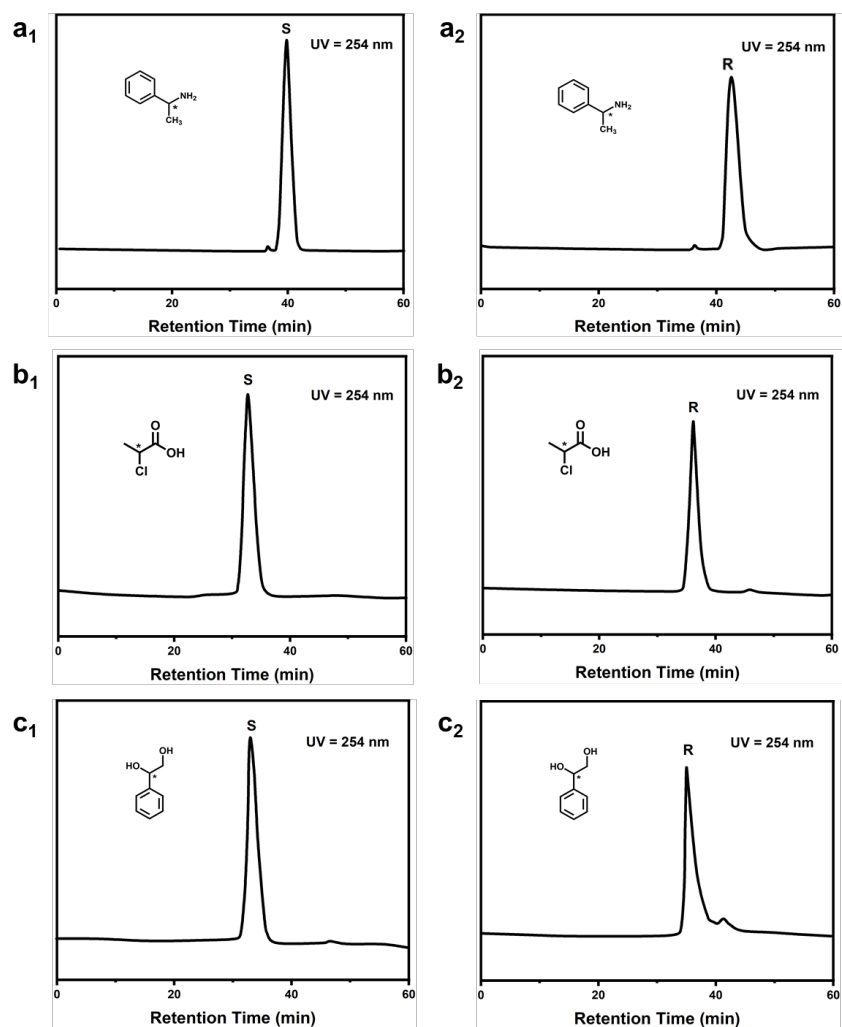


Figure S11. Chromatograms of  $\alpha$ -Phenylethylamine (PA), 2-Chloropropionic acid (CA), 1-Phenyl-1,2-ethanediol (PE) with S-enantiomer and R-enantiomer.

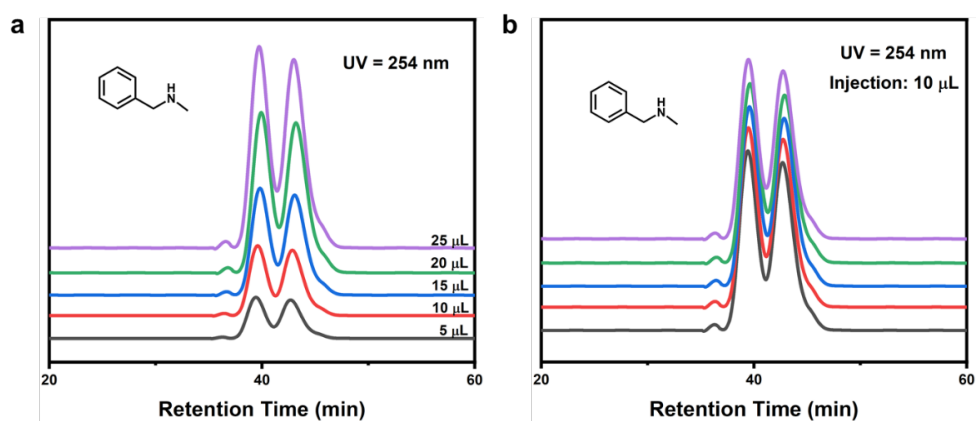


Figure S12. Chromatograms of  $\alpha$ -Phenylethylamine (PA) with different injection volume and five repeated injections.

**Table S1. Comparison of the separation factors among previous published hybrid materials and L-CMHZC@S.**

		PA	PE	CA
CMHZC@S	$k_1$	0.44	0.21	0.20
	$\alpha$	1.28	1.48	1.63
Zr(IV)-MOFs <sup>[1]</sup>	$k_1$			
	$\alpha$	1.38		

[1]. H. Jiang, K. Yang, X. Zhao, W. Zhang, Y. Liu, J. Jiang and Y. Cui, J. Am. Chem. Soc., 2021, 143, 390-398.